

Stimulated Neutrino Transformation Through Turbulence

Kelly M. Patton,^{*} James P. Kneller,[†] and Gail C. McLaughlin[‡]

Department of Physics, North Carolina State University, Raleigh, North Carolina 27695-8202, USA

(Dated: February 28, 2024)

We derive an analytical solution for the flavor evolution of a neutrino through a turbulent density profile which is found to accurately predict the amplitude and transition wavelength of numerical solutions on a case-by-case basis. The evolution is seen to strongly depend upon those Fourier modes in the turbulence which are approximately the same as the splitting between neutrino eigenvalues. Transitions are strongly enhanced by those Fourier modes in the turbulence which are approximately the same as the splitting between neutrino eigenvalues. We also find a suppression of transitions due to the long wavelength modes when the ratio of their amplitude and the wavenumber is of order, or greater than, the first root of the Bessel function J_0 .

PACS numbers: 14.60.Pq

INTRODUCTION

The propagation of neutrinos and their associated flavor transformation is a fascinating problem with many applications. Often neutrinos are propagating through environments where the background potential is not smooth. Examples include propagation through the earth, the sun, supernovae, hypernovae, black hole accretion disks, compact object mergers, and the early universe. Fluctuations can occur on many scales in these complex environments, and it is important to understand which density fluctuation scales will influence neutrino flavor transformation.

There is a long history of research into MSW-type oscillations due to the small scale fluctuations in the earth and sun [1–5], as well as the large, even turbulent fluctuations in supernovae [6–12]. In a supernova environment, neutrino-neutrino interactions must also be considered [13–22]. Recently, the effects of density fluctuations on collective neutrino oscillations have been studied [23–25]. However, in order to fully understand these effects, turbulence and the fluctuation scales which are most important the various types of neutrino oscillations must be identified.

In many of the previous works on neutrino propagation through density fluctuations, either the probability distribution of an ensemble of neutrinos or moments of the distribution [6–9, 26] have been studied. An ensemble consists of neutrinos traveling through many different realizations of turbulence. Under certain conditions such an ensemble will become fully depolarized [27]. In general for N flavors the depolarization limit is where the final distribution of transition probabilities P is proportional to $(1 - P)^{N-2}$ with a mean of $1/N$ [28].

However, it is not always appropriate to use a completely depolarized distribution to characterize the survival probabilities of neutrinos. Depending on the typical history of the neutrinos, it may be better to describe the ensemble with a different distribution, to consider a subset of a distribution through the use of correlations, or to consider individual neutrinos.

Whether considering individual neutrinos, constructing the probability distribution of an ensemble, or computing correlations, the relevant physics is the type and strength of transitions that a neutrino will undergo.

The description of density fluctuations is often a Fourier decomposition into sinusoids, which will produce arbitrarily complicated density distributions depending on the number of modes used. The simplest case is that of a single sinusoidal perturbation super-imposed upon a constant density fluctuation. Neutrinos traveling through this potential can exhibit transitions between states called parametric resonances [29–33]. Parametric resonances are distinct from MSW-type transformations and occur not only when the scale of the sinusoidal fluctuation corresponds to the neutrino mass splitting, but also when it corresponds to harmonics of the mass splitting [12]. A true understanding of which conditions will cause parametric type transitions requires an analytic description of the survival probability of individual neutrinos going through turbulent profiles. In this paper we solve this problem.

We consider neutrino flavor propagation through complicated density profiles, testing examples of up to fifty sinusoids. We first present a numerical flavor transformation calculation through such a profile, then derive an analytic solution for the flavor transformation probability. Comparing this expression to the numerical flavor transformation calculations, we demonstrate that the analytic expression effectively predicts, on a case by case basis, neutrino flavor transformation probabilities as a function of distance. This expression also makes clear the most important density perturbation scales. Not only are the perturbations with wavelengths that correspond to the neutrino mass splitting important, there are additional longer wavelength modes that, if present, can suppress the parametric resonance transitions. This second scale is only weakly dependent on the other scales in the problem, such as δm^2 and the energy of the neutrino. In fact, it depends most strongly on the amplitude of the perturbation. Thus, we show that for any problem involving neutrino flavor transformation through a medium, it is

necessary to understand density fluctuations on two length scales: the scale of the neutrino mass splitting $\lambda_{fluct,split} \sim 20 \text{ km} \left[\left(\left(\frac{\delta m^2}{3 \times 10^{-3} \text{ eV}^2} \right) \left(\frac{20 \text{ MeV}}{E} \right) \left(\frac{\cos 2\theta}{0.95} \right) - 0.53 \left(\frac{\rho}{1000 \text{ g/cm}^3} \right) \right)^2 + 0.1 \left(\left(\frac{\delta m^2}{3 \times 10^{-3} \text{ eV}^2} \right) \left(\frac{20 \text{ MeV}}{E} \right) \left(\frac{\sin 2\theta}{0.3} \right) \right)^2 \right]^{-1/2}$, and the scale that corresponds to the amplitude of the density fluctuations $\lambda_{fluct,ampl} \sim 800 \text{ km} \left(\frac{0.1}{C} \right) \left(\frac{1000 \text{ g/cm}^3}{\rho} \right)$.

A NUMERICAL SOLUTION

The physical quantity we aim to calculate is the probability that an initial neutrino state $|\nu(r)\rangle$ at r is later detected as the state $|\nu'(r')\rangle$ at r' . This probability can be computed from the S -matrix which relates the initial and final neutrino states by the equation $|\nu'(r')\rangle = S(r', r) |\nu(r)\rangle$ [34, 35]. The S -matrix evolves according to the differential equation

$$i \frac{dS}{dr} = H S \quad (1)$$

where H is the Hamiltonian. In the flavor basis H is given by $H^{(f)} = U_0 K_0^{(m)} U_0^\dagger + V^{(f)}$ where U_0 is the vacuum mixing matrix, $K_0^{(m)}$ is the diagonal matrix of vacuum eigenvalues and $V^{(f)}$ some ‘potential’. We shall assume the potential V possesses a ‘smooth’ component, which we denote by \check{V} , and a ‘perturbation’ δV . With this assumption we can regroup the Hamiltonian into $H = \check{H} + \delta V$. We now enforce the requirement that the potential V is ‘MSW’ like in the sense that the only non-zero entry of $V^{(f)}$ is V_{ee} and that the component \check{V}_{ee} is a constant, V_0 . We now focus upon the perturbation and consider the case where δV is built from a series of N_k sinusoidal fluctuations with wavenumbers q_j , amplitudes C_j and phase shifts η_j . Like \check{V} , we restrict ourselves to the case where only δV_{ee} is non-zero. In full the perturbation is written as

$$\delta V_{ee}(r) = V_0 \left\{ \sum_{a=1}^{N_k} C_a \sin(q_a r + \eta_a) \right\} \quad (2)$$

Turbulence is often represented as a Fourier series of exactly this form with realizations generated by assigning random values for the amplitudes, wavenumbers and phase factors according to some algorithm. The phases η_a are typically uniformly distributed from zero to 2π but the random amplitudes and wavenumbers are generated using algorithms that are functions of the power spectrum. Two commonly considered cases are the white-noise power spectrum and the case where the power spectrum is an inverse power law. In figure (1) we show a realization of the white-noise case using $N_k = 50$ where the wavenumbers are uniformly distributed between 0.0045 km^{-1} and 2.2 km^{-1} and the amplitudes are uniformly distributed between 0 and 0.02. The probability we report is the transition probability between the eigenstates of \check{H} . The eigenbasis of \check{H} - which we call the unperturbed matter basis,

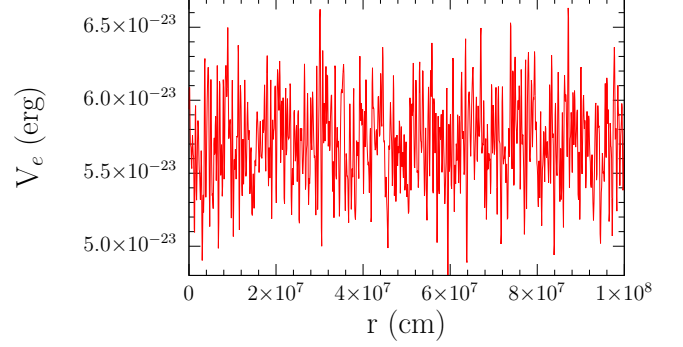


FIG. 1. A turbulent MSW potential. The mean V_0 of the potential is set to be one half the MSW resonance for a 20 MeV neutrino with mixing angle $\sin^2 2\theta = 0.1$ and mass splitting $\delta m^2 = 3 \times 10^{-3} \text{ eV}^2$. The turbulence is composed of $N_k = 50$ sinusoids using the algorithm described in the text.

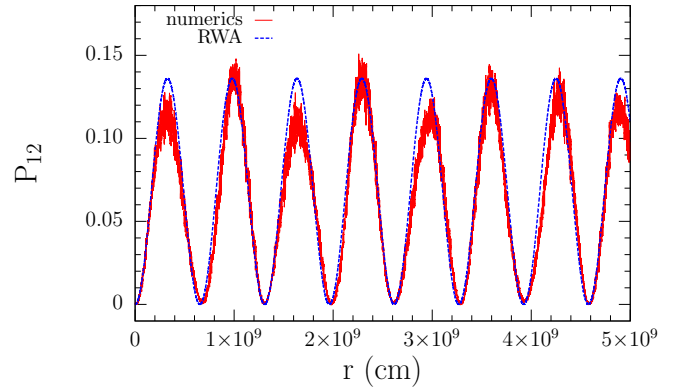


FIG. 2. The numerical solution for the transition probability between the unperturbed neutrino states through the potential shown in figure (1). The sinusoidal curve marked ‘RWA’ is an analytical prediction for the evolution.

denoted by superscript (\check{m}) - is related to the flavor basis by the unitary mixing matrix \check{U} defined by the requirement that it diagonalize $\check{H}^{(f)}$ i.e. $\check{H}^{(f)} = \check{U} \check{K}^{(\check{m})} \check{U}^\dagger$ where $\check{K}^{(\check{m})}$ is the diagonal matrix of eigenvalues, $\check{k}_1, \check{k}_2, \dots$, of \check{H} . Note that the unperturbed matter basis is not equivalent to the instantaneous matter basis. The unperturbed matter basis includes only the ‘smooth’ potential \check{V} , and not the perturbation δV . The unperturbed matter basis is the most suitable basis to calculate the transition probability because transitions vanish when the perturbation vanishes.

The numerical solution for the transition probability for a two-flavor neutrino (we use two-flavors only for the sake of simplicity) with an energy of 20 MeV, vacuum mixing angle of $\sin^2 2\theta = 0.1$ and mass splitting

$\delta m^2 = 3 \times 10^{-3} \text{ eV}^2$, through the turbulence in figure (1) can be observed in figure (2). The mean V_0 of the potential in figure (1) was set to be one half the MSW resonance potential for this energy and mixing parameters. The evolution of P_{12} is really quite remarkable: given the density profile shown in figure (1) one might expect that either the solution for P_{12} would drift gradually to $P_{12} = 0.5$ or that P_{12} would evolve as chaotically as the potential. The actual evolution of P_{12} does neither of these things: it is quasi periodic containing a prominent sinusoidal mode. The curve marked 'RWA' in the figure is a prediction for this component that we now describe.

PREDICTIONS FOR THE WAVELENGTH AND AMPLITUDE

Our analytical treatment for the effect of multiple sinusoidal density fluctuations is a generalization of the treatment presented in Kneller, McLaughlin & Patton [12] for a single sinusoid. Although it is possible to solve this problem with arbitrary numbers of neutrino flavors, we shall restrict ourselves to just two, again, for the sake of clarity. Our first step is to transform the problem into the unperturbed matter basis using the mixing matrix \tilde{U} . After this transformation, the Hamiltonian is written as

$$H^{(\tilde{m})} = \tilde{K}^{(\tilde{m})} - i\tilde{U}^\dagger \frac{d\tilde{U}}{dr} + \tilde{U}^\dagger \delta V^{(f)} \tilde{U}. \quad (3)$$

We write the S -matrix for the unperturbed matter basis as the product $S^{(\tilde{m})} = \tilde{S} A$ where \tilde{S} is solution of the unperturbed problem i.e. the constant density Hamiltonian \tilde{H} , defined by the equation

$$i \frac{d\tilde{S}}{dr} = \left[\tilde{K}^{(\tilde{m})} - i\tilde{U}^\dagger \frac{d\tilde{U}}{dr} \right] \tilde{S}. \quad (4)$$

Note that we have suppressed the factors of $\hbar c$ that occur in the S -matrix equation.

For this potential \tilde{S} is simply $\tilde{S} = \exp(-i\tilde{K}^{(\tilde{m})} x)$ because the eigenvalues of \tilde{H} are constant. Since \tilde{S} is known we can solve for the effect of the perturbation δV by finding the solution for A , given by the differential equation

$$i \frac{dA}{dr} = \tilde{S}^\dagger \tilde{U}^\dagger \delta V^{(f)} \tilde{U} \tilde{S} A. \quad (5)$$

The Hamiltonian for A possesses both diagonal and off-diagonal elements but those diagonal elements can be removed by writing the matrix A as $A = W B$ where $W = \exp(-i\Xi)$ and Ξ is a diagonal matrix $\Xi = \text{diag}(\xi_1, \xi_2)$, see [12]. Using equation (5), we find the differential equation for B is

$$i \frac{dB}{dr} = W^\dagger \left[\tilde{S}^\dagger \tilde{U}^\dagger \delta V^{(f)} \tilde{U} \tilde{S} - \frac{d\Xi}{dr} \right] W B, \quad (6)$$

where the diagonal matrix Ξ is chosen in order to remove the diagonal elements of $\tilde{S}^\dagger \tilde{U}^\dagger \delta V^{(f)} \tilde{U} \tilde{S}$.

The quantities ξ_i using our form for δV are

$$\xi_i = V_0 |\tilde{U}_{ei}|^2 \left\{ \sum_{a=1}^{N_k} \frac{C_a}{q_a} [\cos \eta_a - \cos(q_a r + \eta_a)] \right\}. \quad (7)$$

Using this result, the equation for dB/dx is found to be

$$i \frac{dB}{dx} = V_0 \left\{ \sum_{a=1}^{N_k} C_a \sin(q_a r + \eta_a) \right\} \begin{pmatrix} 0 & \tilde{U}_{e1}^* \tilde{U}_{e2} e^{i(\delta \tilde{k}_{12} r + \delta \xi_{12})} \\ \tilde{U}_{e2}^* \tilde{U}_{e1} e^{-i(\delta \tilde{k}_{12} r + \delta \xi_{12})} & 0 \end{pmatrix} B \quad (8)$$

where $\delta \tilde{k}_{12} = \tilde{k}_1 - \tilde{k}_2$ and similarly $\delta \xi_{12} = \xi_1 - \xi_2$. The next step is to use the Jacobi-Anger expansion for the complex exponentials $\exp(i\delta \xi_{12})$

$$\exp(i\delta \xi_{12}) = \prod_{a=1}^{N_k} \sum_{n_a=-\infty}^{\infty} (-i)^{n_a} J_{n_a}(z_a) \times \exp[i z_a \cos \eta_a + i n_a (q_a r + \eta_a)] \quad (9)$$

where J_n is the Bessel J function and, in order to tidy up the notation, we have introduced the quantities z_a defined to be

$$z_a = \frac{C_a V_0}{\hbar c q_a} (|\tilde{U}_{e1}|^2 - |\tilde{U}_{e2}|^2). \quad (10)$$

In Eq. 10 we have added back in the factor of $\hbar c$. The Jacobi-Anger expansion is really a Fourier series expansion, where each term has a coefficient $(-i)^{n_a} J_{n_a}(z_a) \exp[i z_a \cos \eta_a]$. For $n = 0$, this coefficient is simply the mean value of the complex exponential.

Using this expansion and the definition we find

$$i \frac{dB}{dx} = \begin{pmatrix} 0 & h_{12} \\ h_{21} & 0 \end{pmatrix} B \quad (11)$$

where the elements h_{12} and h_{21} are given by

$$h_{12} = h_{21}^* = \frac{\tilde{U}_{e1}^* \tilde{U}_{e2}}{|\tilde{U}_{e1}|^2 - |\tilde{U}_{e2}|^2} \sum_{a=1}^{N_k} \sum_{n_a=-\infty}^{+\infty} n_a q_a \kappa_{a,n_a} \quad (12)$$

$$\prod_{b=1, b \neq a}^{N_k} \left\{ \sum_{n_b=-\infty}^{+\infty} \kappa_{b,n_b} \exp[i(\delta \tilde{k}_{12} + n_a q_a + n_b q_b) r] \right\}$$

with the complex parameters κ_{a,n_a} defined to be

$$\kappa_{a,n_a} = (-i)^{n_a} J_{n_a}(z_a) \exp[i(n_a \eta_a + z_a \cos \eta_a)]. \quad (13)$$

Note that part of the definition of κ is the coefficient from the Jacobi-Anger expansion. This form for the components of the Hamiltonian closely matches that found for similar systems in molecular physics, such as that studied in Kondo, Blokker, & Meath [36].

To make additional progress we make use of the Rotating Wave Approximation (RWA) and drop all terms in each infinite series - the n_a 's and n_b 's - in equation (12) except the most 'important'. The most important set of integers can be found from the criterion used for the case of a single sinusoidal perturbation. We select the values for the n_a 's

which come closest to satisfying the parametric resonance condition $|\delta k_{12} + \sum_a n_a q_a| \approx 0$. We denote these values by $n_{\star a}$. The RWA removes the sum over each n_a and n_b and we can define the quantity

$$\kappa = \frac{\check{U}_{e1}^* \check{U}_{e2}}{|\check{U}_{e1}|^2 - |\check{U}_{e2}|^2} \left(\sum_{a=1}^{N_k} n_{\star a} q_a \right) \prod_{a=1}^{N_k} \kappa_{a, n_{\star a}} \quad (14)$$

After making the RWA we can write out the solution for B after introducing $2p = \delta k_{12} + \sum_a n_{\star a} q_a$ and $Q^2 = p^2 + \kappa^2$, see Kneller, McLaughlin & Patton [12].

The RWA allows us to write the differential equation for B as

$$\iota \frac{dB}{dr} = H^{(B)} B, \quad (15)$$

and define the RWA Hamiltonian as

$$H^{(B)} = \begin{pmatrix} 0 & \kappa \exp(2\iota p r) \\ \kappa^* \exp(-2\iota p r) & 0 \end{pmatrix}. \quad (16)$$

Following the procedure outlined in [12], we find the solution for B is

$$B = \begin{pmatrix} e^{\iota p r} \left[\cos(Qr) - \iota \frac{p}{Q} \sin(Qr) \right] & -\iota e^{\iota p r} \frac{\kappa}{Q} \sin(Qr) \\ -\iota e^{-\iota p r} \frac{\kappa^*}{Q} \sin(Qr) & e^{-\iota p r} \left[\cos(Qr) + \iota \frac{p}{Q} \sin(Qr) \right] \end{pmatrix}. \quad (17)$$

Since we assumed the unperturbed potential was a constant, the unperturbed matrix \check{S} and the matrix W are diagonal matrices, so we find that the transition probability between the unperturbed matter states 1 and 2 is of the form

$$P_{12} = |B_{12}|^2 = \frac{\kappa^2}{Q^2} \sin^2(Qr). \quad (18)$$

In practice we found that when the number of sinusoids N_k is large it is computationally prohibitive to locate the values of the N_k integers which minimize the phase $|\delta k_{12} + \sum_a n_a q_a|$ via a scan. When N_k is large our strategy for locating the RWA solution is to use $-\kappa^2/Q^2$, or the negative of the amplitude, as a ‘potential’ in the N_k dimensional space of integers and then locate the minimum of the potential using a simplex. The RWA solution for the turbulence shown in figure (1) - using the simplex algorithm to locate the integers - is the second solution shown in figure (2) marked ‘RWA’. The reader will observe that it is a good description of both the amplitude and the wavelength of the dominant sinusoidal component of P_{12} .

SUPPRESSED TRANSITIONS

The success of the RWA solution shown in figure (2) indicates the theory describes the overall features of the numerical solution well. The RWA solution obviously depends upon those wavenumbers with non-zero contributions to fulfilling the parametric resonance condition

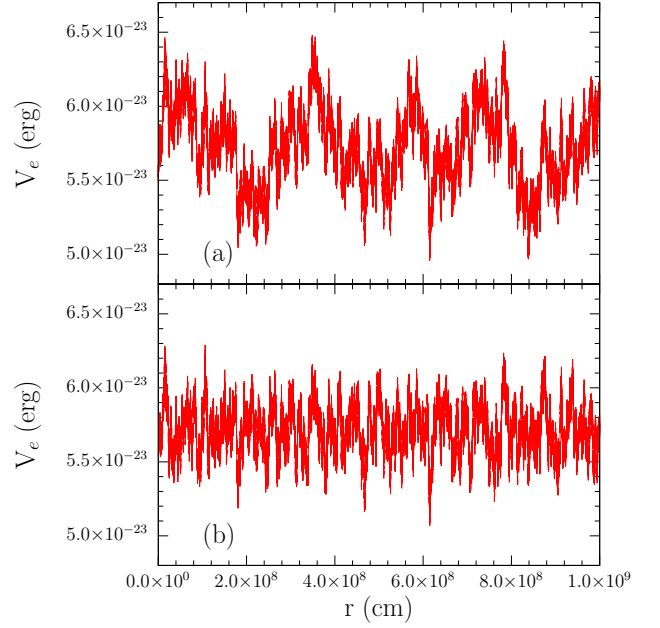


FIG. 3. Two turbulent neutrino potentials. In the upper panel the realization is uses an inverse power law spectrum. The lower panel is the exact same set of amplitudes, wavenumbers and phases as the upper panel but with the five lowest wavenumbers removed.

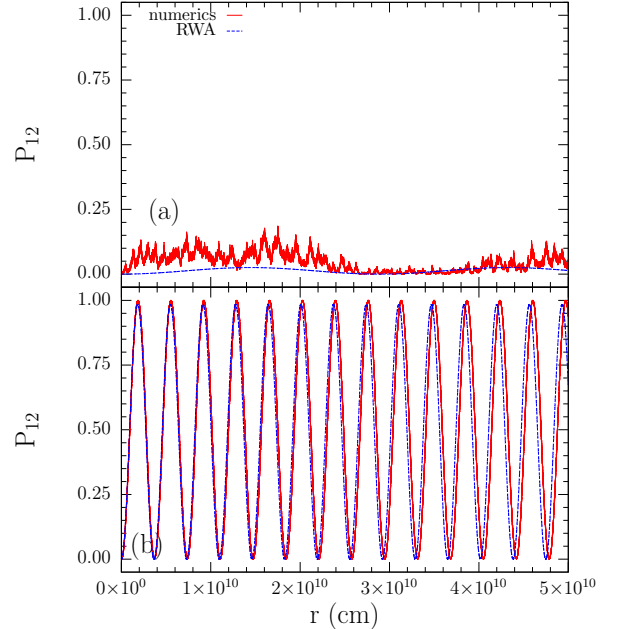


FIG. 4. The numerical and analytical solutions for the neutrino evolution through the turbulent potentials shown in figure (3).

$\delta\check{k}_{12} + \sum_a n_a q_a \approx 0$. Defining $\lambda_{fluct,split} \sim 2\pi/q_a$ for these modes, we find the scale given in the introduction. But that is not the whole story: the quantity κ , which controls the amplitude and the wavelength of the transitions, actually depends upon every wavenumber even if the RWA solution indicates it does so with $n_{\star a} = 0$.

To understand this effect, consider equation (8). We can break the matrix elements of the Hamiltonian in this equation into three parts. The coefficient of the exponential, $\check{U}_{e1}^\star \check{U}_{e2} V_0 \left\{ \sum_{a=1}^{N_k} C_a \sin(q_a r + \eta_a) \right\}$, or the complex conjugate, is an operator which connects the two neutrino states. The complex exponential $e^{i\delta k_{12} r}$ is the unperturbed solution to the problem and it describes the evolution of the neutrinos in the constant density potential. Finally, the complex exponential $e^{i\delta\xi_{12}}$ is the distortion to the unperturbed solution by the diagonal elements of δV . This distortion reflects the modification of oscillation frequency of the unperturbed system. As we discuss in the following paragraphs, the modes which cause the parametric resonance transitions create little change in this frequency, but longer wavelength modes can create larger changes.

This term can be written as a product of the distortions from each individual mode:

$$e^{i\delta\xi_{12}} = \prod_{a=1}^{N_k} e^{i\delta\xi_{12a}}, \quad (19)$$

Recall that in deriving the solution 18 we expanded each $e^{i\delta\xi_{12a}}$ using the Jacobi-Anger expansion 9, and retained only the relevant $n_{\star a}$ term. For the modes which don't contribute to the parametric resonance, this is the $n_{\star a} = 0$ term. Through an identity of Bessel functions this term can be written as

$$J_0(z_a) \exp[i z_a \cos \eta_a] = \langle e^{i\delta\xi_{12a}} \rangle, \quad (20)$$

where the average value is defined explicitly as

$$\langle e^{i\delta\xi_{12a}} \rangle = \frac{2\pi}{q_a} \int_0^{2\pi/q_a} dr e^{i\delta\xi_{12a}}. \quad (21)$$

Thus for all the modes that don't contribute to the parametric resonance, each distortion can be represented by an average value and the oscillatory terms in the Jacobi-Anger expansion in equation (9) can be neglected. As long as the average value of the distortion, $J_0(z_a)$, for all these modes is close to unity, then these modes which don't contribute to the parametric resonance make only small modifications to the amplitude and wavelength of the solution 18. But when the average value of the distortion is large, i.e. $|J_0(z_a)| < 1$, then these modes can significantly modify they amplitude and wavelength of the solution even though they do not contribute to the parametric resonance!

Examining the argument of the Bessel function, $z_a \sim C_a V_0/(\hbar c q_a)$, we see that the criteria for determining whether a mode causes significant distortion is the ratio of its amplitude to its wavenumber. As long as the fluctuation amplitude $C_a V_0/(\hbar c)$ is much smaller than the wavenumber q_a , then $\langle e^{i\delta\xi_{12a}} \rangle \sim 1$, and that mode will cause little

distortion. However, if $z_a \sim C_a V_0/(\hbar c q_a) > 1$ then the value of the Bessel function will be small and there will be considerable distortion, $\langle e^{i\delta\xi_{12a}} \rangle < 1$. In addition, if there is a mode for which the value of z_a hits a zero of a Bessel function then there is maximal distortion $\langle e^{i\delta\xi_{12a}} \rangle \sim 0$. In these situations, the transitions are extraordinarily strongly suppressed since the distortion of all the modes appears as a multiplicative factor.

We can identify the largest wavenumbers which cause significant distortion by examining the point where $J_0(z_a)$ hits its first zero, the first of which occurs when $z_a \sim 2.4$. Using equation (10), we find the wavenumbers of interest by setting $z_a \sim C_a V_0/(\hbar c q_a) \sim 2.4$. If we define $\lambda_{fluct,ampl} \sim 2\pi/q_a$ for these modes, we find the expression given in the introduction. From the scaling of z_a with q_a we discover it is the long wavelength modes which dominate this effect, not the small wavelengths.

We show this dependence upon the long wavelength turbulence modes by generating the two turbulence density profiles shown in figure (3) using an inverse power law spectrum (see [26, 37, 38] for a description of the algorithm we use for this case) with the rms amplitude of the turbulence set to 0.05, a spectral index of $\alpha = 5/3$, and a long wavelength cutoff set to ~ 3000 km. Since V_0 is only half the MSW density, it is would require an extremely unlikely, $20 - \sigma$, fluctuation to approach the MSW density with this turbulence amplitude. After generating the turbulence, we slightly increased the wavelength and amplitude of the longest wavelength mode by hand to give $z_1 \sim 2.4$. The only difference between the two profiles is that the five longest wavelength modes from the top panel have been removed for the lower. The missing modes possess wavenumbers many orders of magnitude smaller than the eigenvalue splitting $\delta\check{k}_{12}$. The RWA solution for these realizations are found to be $n_{\star a} = 0$ for every mode, including the five longest wavelengths, except for one mode which happens to satisfy the parametric resonance condition by itself. If there were no dependence upon the wavelengths where $n_{\star a} = 0$ then removing the five longest wavelength modes should not change the solution. However, when we actually solve for P_{12} with and without these five wavelengths we do find different solutions as shown in figure (4). Note that the horizontal scale on the figure is more than one hundred times larger than the longest wavelength mode in the turbulence i.e. the cutoff. Without the five longest wavelengths the amplitude of the transition is unity and the wavelength of order $\sim 3 \times 10^9$ cm: with the five longest wavelengths the amplitude is only ~ 0.1 and the wavelength stretches to $\sim 3 \times 10^{10}$ cm.

Inspection of the values of z_a for the five modes indicates they all lie in the vicinity of the first root of J_0 . The distortion predicted from these five modes together, obtained by multiplying the individual distortions given by equation (20), is ~ 0.02 . This is mainly due to the first mode, which had $z_1 \sim 2.4$, although the other four missing modes also contribute. Even though these five modes all have $n_{\star a} = 0$,

they still have a strong effect on the transition.

The example shown in figure (4) was specifically tailored to show how dramatic the suppression effect can be. However, we also found that it occurs in more general examples. Using a white noise spectrum with wavelengths between 3 km and 300 km and amplitudes up to 0.025, 20 examples with $N_k = 20$ where a parametric resonance occurred were found. We added $N_k = 20$ extra modes with wavelengths between 300 km and 3000 km, then 300 km to 30000 km, to those original white noise spectra. This resulted in perturbations with $N_k = 40$ that were known to have a parametric resonance, but also had the possibility of exhibiting suppression. In approximately half of the trials, the amplitudes found in the numeric simulations showed suppression varying from just a few percent to almost 50%. From these results, we expect that suppression will occur for approximately half of turbulent spectra, with the degree of suppression depending on the values of wavelength and corresponding amplitudes within the spectrum.

Finally, we note the analogy, with the Stark effect for a two-level atom. For a two-level atom, transitions are stimulated between the states by a laser if the laser frequency matches the energy splitting of the system. Placing the atom in an external electric field causes shifts in the wave functions and energies of the original (unperturbed) states. Once this shift occurs, a laser that stimulated transitions prior to the application of the electric field can no longer do so. In the neutrino case, the “lasers” are the modes fulfilling the parametric resonance condition, and the external electric field corresponds to modes with $n_{\star a} = 0$.

CONCLUSIONS

Understanding neutrino propagation through turbulent media is essential to understanding future measurements of supernova neutrino spectra. While previous treatments have focused primarily on the behavior of ensemble averages, we have instead considered the exact propagation of single neutrinos. Our analytic results show that density perturbations play two roles. We confirm that density perturbations can cause transition between states. Even in very complicated density profiles the density fluctuations that occur on wavelengths that match the natural wavelength of the neutrinos cause the biggest transition. However, we find that longer wavelength density fluctuations also *suppress* transitions. They do so by causing the basis state to significantly fluctuate away from its original state on scales shorter than the parametric resonance transition.

A clear implication of these results is that in any environment where neutrinos propagate, it is important to understand the density fluctuations both on the scale of the effective mass splitting and on the scales where the amplitude of the fluctuation corresponds to its wavenumber. Together with the results presented in this paper, this information can be used to determine the strength and number of transitions

a neutrino will experience as it passes through a turbulent ensemble. This aids in determining the applicability of the depolarization limit of an ensemble of neutrinos.

Many environments have non-constant base density profiles. To make useful predictions in environments such as supernovae, extensions beyond the constant base profile must be considered.

This work was supported by DOE grants DE-SC0004786 (GCM+JPK+KMP) and DE-SC0006417 (JPK), DE-FG02-02ER41216 (GCM+KMP) and by a NC State University GAANN fellowship (KMP). The authors would also like to thank William Meath for useful discussions.

* kmpatton@ncsu.edu

† jim_kneller@ncsu.edu

‡ gail_mclaughlin@ncsu.edu

- [1] W. C. Haxton and W. M. Zhang 1991 Phys. Rev. **D43** 2484
- [2] T. Ohlsson and H. Snellman 2001 European Physical Journal C **20** 507
- [3] H. Nunokawa, A. Rossi, V. B. Semikoz and J. W. F. Valle, 1996 Nucl. Phys. **B472** 495
- [4] C. P. Burgess and D. Michaud, 1997 Annals Phys. **256** 1
- [5] R. F. Sawyer, 1990 Phys Rev. **D42** 3908
- [6] F. N. Loreti, Y. Z. Qian, G. M. Fuller and A. B. Balantekin, Phys. Rev. D **52** 6664 (1995)
- [7] A. Friedland and A. Gruzinov, astro-ph/0607244.
- [8] G. Fogli, E. Lisi, A. Mirizzi and D. Montanino, 2006 J. Cosmol. Astropart. Phys. **06** 012
- [9] J. P. Kneller, and C. Volpe, Phys. Rev. D **82** 123004 (2010)
- [10] E. Boriello, S. Chakraborty, H.-T. Janka, E. Lisi and A. Mirizzi, 2013 arXiv:1310.7488v1 [astro-ph]
- [11] S. Choubey, N. P. Harries and G. .G. Ross, 2007 Phys. Rev. **D76** 073013
- [12] J. P. Kneller, G. C. McLaughlin and K. M. Patton, J. Phys. G **40** 055002 (2013)
- [13] Y. -Z. Qian and G. M. Fuller, Phys. Rev. **D52**, 656 (1995)
- [14] G. M. Fuller and Y. -Z. Qian, Phys. Rev. **D73**, 023004 (2006)
- [15] H. Duan, G. M. Fuller, J. Carlson and Y. -Z. Qian, Phys. Rev. **D74**, 105014 (2006)
- [16] A. B. Balantekin and Y. Pehlivan, J. Phys. G **34**, 47 (2007)
- [17] H. Duan, G. M. Fuller and Y. -Z. Qian, Phys. Rev. **D76**, 085013 (2007)
- [18] H. Duan, G. M. Fuller, J. Carlson and Y. -Z. Qian, Phys. Rev. Lett. **97** (2006) 241101
- [19] H. Duan, G. M. Fuller and Y. -Z. Qian, Ann. Rev. Nucl. Part. Sci. **60**, 569 (2010)
- [20] J. Gava, J. Kneller, C. Volpe and G. C. McLaughlin, Phys. Rev. Lett. **103**, 071101 (2009)
- [21] A. Esteban-Pretel, S. Pastor, R. Tomas, G. G. Raffelt and G. Sigl, J. Phys. Conf. Ser. **120**, 052021 (2008)
- [22] A. Banerjee, A. Dighe and G. Raffelt, Phys. Rev. **D84**, 053013 (2011)
- [23] G. Reid, J. Adams and S. Seunarine 2011 Phys. Rev. **D84** 085023
- [24] J. F. Cherry, M.-R. Wu, J. Carlson, H. Duan, G. M. Fuller,

- and Y.-Z. Qian, 2011 Phys. Rev. **D84** 105034
- [25] J. F. Cherry, M.-R. Wu, J. Carlson, H. Duan, G. M. Fuller, and Y.-Z. Qian, 2011, arXiv:1109.5195v1
- [26] J. P. Kneller and A. W. Mauney, Phys. Rev. D **88** 025004 (2013)
- [27] Loreti F N and Balantekin A B 1994 Phys. Rev. D **50** 4762
- [28] Kneller J P Preprint arXiv:1004.1288 [hep-ph]
- [29] V. K. Ermilova, V. A. Tsarev and V. A. Chechin, 1986 Kr. Soob, Fiz. Lebedev Institute **5** 26
- [30] A. Schäfer and S. E. Koonin, 1987 Phys. Lett **B185** 417
- [31] E. K. Akhmedov, 1988 Sov. J. of Nuclear Physics **47** 301, Yad. Fiz **47** 475
- [32] P. I. Krastev, and A. Y. Smirnov, 1989 Phys. Lett **B226** 341
- [33] M. Koike, T. Ota, M. Saito and J. Sato, 2009 Phys.Lett. **B675** 69
- [34] J. P. Kneller and G. C. McLaughlin, Phys. Rev. **D 73** 056003 (2006)
- [35] J. P. Kneller and G. C. McLaughlin, Phys. Rev. **D 80**, 053002 (2009) [arXiv:0904.3823v1]
- [36] A. E. Kondo, V. M. Blokker, and W. J. Meath, J. Chem. Phys. **96** (4) 2544 (1992)
- [37] J. P. Kneller and A. W. Mauney, , Phys. Rev. D, **88**, 045020 (2013)
- [38] T. Lund, and J. P. Kneller, Phys. Rev. D **88** 023008 (2013)